Article

Not peer-reviewed version

Possibilities of Duplex Plasma Electrolytic Treatment for In-Creasing the Hardness and Wear Resistance of the CP-Ti Surface

Sergei Kusmanov *, Tatiana Mukhacheva, Ivan Tambovskiy, Irina Kusmanova, Sergei Shadrin, Roman Belov, Roman Nikiforov, Igor Suminov, Mikhail Karasev, Sergey Grigoriev

Posted Date: 21 June 2023

doi: 10.20944/preprints202306.1529.v1

Keywords: plasma electrolytic nitrocarburising; plasma electrolytic polishing; CP-Ti; friction; wear; microhardness; roughness

Article

Possibilities of Duplex Plasma Electrolytic Treatment for Increasing the Hardness and Wear Resistance of the CP-Ti Surface

Sergei Kusmanov [1,*], Tatiana Mukhacheva [1,2], Ivan Tambovskiy [1,2], Irina Kusmanova [1], Sergei Shadrin [1], Roman Belov [1], Roman Nikiforov [1], Igor Suminov [2], Mikhail Karasev [3] and Sergey Grigoriev [2]

[1] Department of Mathematical and Natural Sciences, Kostroma State University, 156005 Kostroma, Russia; mukhachevatl@mail.ru (T.M.); ramstobiliti@gmail.com (I.T.); maly.s@rambler.ru (I.K.); syushadrin@yandex.ru (S.S.); solne4nyjkrug@bk.ru (R.B.); chost0848@gmail.com (R.N.)

[2] Department of High-Efficiency Machining Technologies, Moscow State University of Technology "STANKIN", 127994 Moscow, Russia; ist3@mail.ru (I.S.); sngrig@mail.ru (S.G.)

[3] Department of Management and Law, Kostroma State Agricultural Academy, 156530, Kostroma region, Karavaevo, Russia; mihail.karasev.1983@mail.ru

* Correspondence: sakusmanov@yandex.ru; Tel.: +7-920-6473-090

Abstract: The possibility of increasing wear resistance of the CP-Ti surface using a duplex surface treatment combining plasma electrolytic nitrocarburizing in a solution of ammonia, acetone and ammonium chloride and subsequent plasma electrolytic polishing is shown. Morphology and surface roughness, structure and microhardness of the modified layer were studied. The correlation of weight wear with hardness of diffusion layer at a low processing temperature and thickness of oxide layer is established – the largest decrease in weight wear occurs after nitrocarburizing at 750 °C for 5 min (by 4.3 times). The possibility of an additional increase in wear resistance by subsequent polishing of the nitrocarburized CP-Ti surface at a voltage of 275–300 V for 3–5 min in chloride and fluoride electrolytes and 5–10 min in a sulfate electrolyte was revealed. Under these conditions, the hardened layer is preserved when the porous outer oxide layer is removed. According to the microtopology of the friction tracks, the wear mechanism is estimated as fatigue in dry friction and plastic contact.

Keywords: plasma electrolytic nitrocarburising; plasma electrolytic polishing; CP-Ti; friction; wear; microhardness; roughness

1. Introduction

Titanium alloys play an important role in the development of products of a variety of uses. In a number of cases, titanium-based materials are indispensable in shipbuilding and industry – they are used to produce parts used to work with aggressive liquids, in corrosive environments, and when anodizing various parts. Promising industries in which it is advisable to use materials based on titanium are nuclear power, oil and gas production, and non-ferrous metallurgy. Alloyed materials with high performance indicators are generally used for critical parts. At the same time, surface treatment of a finished product can be an alternative to increase the functional performance. Modifying product surfaces of low-grade alloys in areas of contact with the external environment allows the use of cheaper materials while increasing performance indicators. To harden metal surfaces, plastic deformation technologies, for example, ultrasonic strain engineering technology [1] and ultrasonic shot peening [2,3]. The disadvantage of deformation treatments is the significant increase in roughness and the need for subsequent finishing [1–3].

An alternative method of modifying metal and alloy surfaces to increase a variety of performance indicators is plasma electrolytic treatment [4–7]. There is a variety of processes aimed at obtaining ceramic-like coatings by plasma electrolytic oxidation [8–10], surface polishing or removal of the surface layer by plasma electrolytic polishing [11], but also surface modification

 doi:10.20944/preprints202306.1529.v1

through plasma electrolytic diffusion hardening [12–15], which has found a wide application for processing of steel products.

Cathodic plasma electrolytic nitriding of medium carbon steel S0050A leads to an increase in the dry friction coefficient from 0.37 to 0.4, and also from 0.109 to 0.125 when using a lubricant [16]. A possible reason for this is the increase in the surface roughness. At the same time, an increase in hardness secures a three-fold decrease in volume wear resulting in dry friction. Cathodic boriding of H13 steel improves wear resistance by a factor of 12 when conducting abrasive wear 'finger-on-disk' tests with a silicon carbide counterbody [17]. Anodic boriding of medium carbon steel in dry friction setting makes it possible to increase the wear resistance by a factor of 7.2 while decreasing the friction coefficient from 0.26 to 0.16 [18]. The formation of hardening borides and martensite after anodic boriding of carbon steel 45 leads to a 16-fold increase in wear resistance in dry friction and two-fold in lubricated friction due to a significant increase in hardness and a decrease in surface roughness [19].

Plasma electrolytic diffusion saturation of titanium alloys also has known advantages. It has been established that with the help of cathodic plasma electrolytic saturation with nitrogen and carbon, it is possible to increase the hardness of commercial titanium (CP-Ti) up to 800 HV using an aqueous solution of carbamide and sodium carbonate [20], or up to 1500 HV in a solution of carbamide, triethanolamine and formamide [21]. The hardness of the Ti6Al4V alloy after nitrocarburizing in a solution of ammonium nitrate, ethanol, and glycerol reaches 2000 HV [22], and in a solution of triethanolamine and formamide, 2369 HV [23]. Such treatment makes it possible to reduce the weight wear of CP-Ti 17-fold [20], and Ti6Al4V 3248-fold. [23]. In [24], the complex effect of surface roughness and hardness of the surface layer on the wear resistance of Ti6Al4V titanium alloy after cathodic nitriding has been established. It has been established that the largest decrease in mass wear of 2.7-fold is observed in specimens with the maximum microhardness of the surface layer, reaching 820 HV, and the lowest surface roughness. It has also been shown that pulse saturation of titanium with nitrogen and carbon leads to the formation of nanocrystalline carbonitrides [25] and an increase in the corrosion resistance of CP-Ti after nitrocarburizing in triethanolamine [26] or in a mixture of carbamide, triethanolamine and formamide [21].

A noted disadvantage of the cathodic version of plasma electrolytic diffusion saturation is surface erosion resulting from electric discharges, leading to crater and irregularities formation on the surface and an increase in its roughness [27]. A disadvantage of the anodic saturation technology is the formation of porous oxide structures on the surface [28,29], which can peel off when interacting with external objects, wear out easily with friction, and destroy the surface like an abrasive. One of the solutions to these problems is the subsequent plasma electrolytic polishing (PEP) after diffusion saturation, allowing to remove a part of the surface oxide layer with the formed defects and further reduce the surface roughness. In this regard, the purpose of this work is to study the possibility of increasing the wear resistance of a titanium surface by combined plasma electrolytic treatment by nitrocarburizing and polishing.

2. Materials and Methods

2.1. Samples Processing

Cylindrical samples (∅ 10 mm × 15 mm) of CP-Ti (0.25 wt.% Fe; 0.2 wt.% O, 0.1 wt.% Si; 0.07 wt.% C; 0.04 wt.% N; 0.01 wt.% H, and balanced Ti) were ground with SiC abrasive paper to a grit size of P120 to Ra~1.0 μm and ultrasonically cleaned with acetone. These samples were subjected to duplex surface treatment combining plasma electrolytic nitrocarburizing (PENC) in a solution of ammonia (5 wt.%), acetone (5 wt.%) and ammonium chloride (10 wt.%) and subsequent PEP.

Plasma electrolytic treatment was carried out in a cylindrical electrolyzer with an axially symmetric electrolyte flow supplied through a nozzle located at the bottom of the electrolyzer (Figure 1) [30].

Preprints (www.preprints.org) | NOT PEER-REVIEWED | Posted: 21 June 2023 doi:10.20944/preprints202306.1529.v1

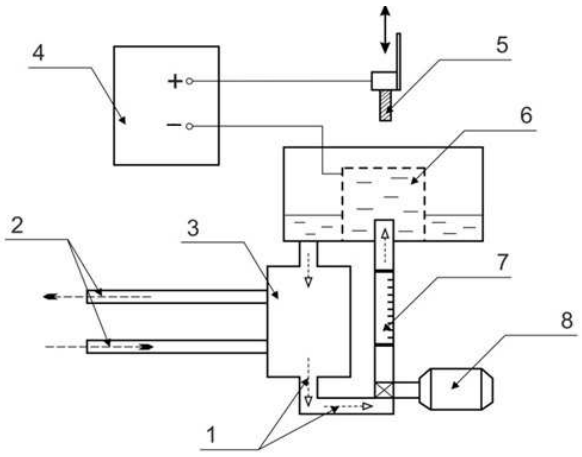

Figure 1. Schematic diagram for plasma electrolytic treatment: 1—electrolyte; 2—cold water; 3—heat exchanger; 4—power supply; 5—treated sample; 6—electrolytic cell; 7—flowmeter; 8—pump.

In the upper part of the electrolyzer, electrolyte was overflowing into the sump and was further pumped through a heat exchanger at a rate of 2.5 L/min, which was measured with a 0.4–4 LPM flowmeter (accuracy of ± 2.5%) (Pribormarket, Arzamas, Russia). This scheme provides stabilization of the processing conditions. Solution temperature was measured using a a K-type thermocouple (Termoelement, Moscow, Russia) placed at the bottom of the chamber and maintained at 30 ± 2 °C. The samples were connected as the positive output, and the electrolyzer (Figure 1) was connected as the negative output of the 15 kW DC power supply. The PENC time was 5 min as the most optimal for anodic variants of plasma electrolytic treatment [31–33]. PENC was carried out at temperatures of 750, 800, 850, and 900 °C by changing the voltage according to the voltage-temperature characteristic of the process (Figure 2). After PENC, the samples were quenched in the electrolyte (hardening).

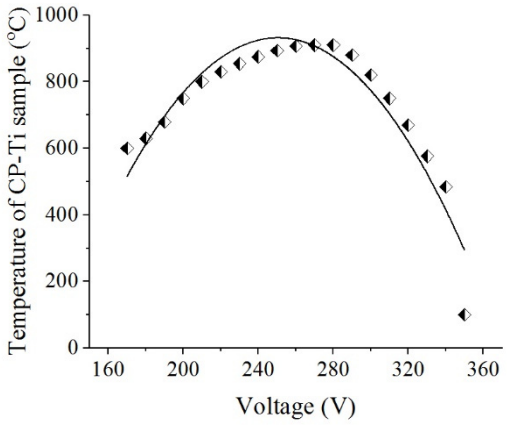

Figure 2. The voltage-temperature characteristic of PENC.

Following PENC, the samples were subjected to subsequent PEP in different solutions: ammonium sulfate (3%) at a temperature of 80 °C; ammonium chloride (1%) at a temperature of 80 °C; and ammonium fluoride (4%) at a temperature of 90 °C, with varying voltage and time processing. The electrolyte was pumped through a heat exchanger at a flow rate of 1 L/min.

2.2. Study of the Surface Morphology and Microstructure

 doi:10.20944/preprints202306.1529.v1

The Phenom g2 pro scanning electron microscope (Phenom-World B.V., Eindhoven, The Netherlands) with digital image visualization served to study the surface morphology and microstructure of the cross-section of the CP-Ti samples.

The Micromed MET (Micromed, St. Petersburg, Russia) optical metallographic microscope with digital image visualization served to study the surface morphology of the CP-Ti samples.

2.3. The Microhardness Measurement

The microhardness of the cross-sections of the treatment sample was measured using a Vickers microhardness tester (Falcon 503, Innovatest Europe BV, Maastricht, The Netherlands) under a 0.1 N load. According to 5 measurements, the average value of microhardness was found.

2.4. Surface Roughness and Weight of Samples Measurement

The surface roughness was measured with a TR-200 profilometer (Beijing TIME High Technology Ltd., Beijing, China). According to 10 measurements, the average value of roughness indicators was found. The change in the weight of the samples was determined on a CitizonCY224C electronic analytical balance (ACZET (Citizen Scale), Mumbai, India) with an accuracy of ± 0.0001 g after removing traces of salts by washing the samples in distilled water and subsequently drying.

2.5. Study of Tribological Properties

The friction scheme "shaft-block" was used in friction tests (Figure 3) [31,34].

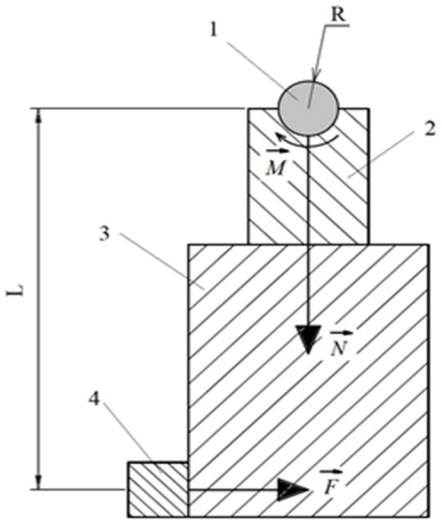

Figure 3. Friction scheme. 1—sample; 2—counter body; 3—pendulum; 4—strain gauge. *M*—frictional moment; *N*—force acting on the counter body and the pendulum from the side of the sample; *F*—force acting on the pendulum from the strain gauge; *L*—distance from the axis of rotation to the axis of symmetry of the strain gauge, *R* – radius of the sample.

The counter body was made of tool alloy steel (wt.%: 0.9–1.2 Cr, 1.2–1.6 W, 0.8–1.1 Mn and 0.9–1.05 C) in the form of a plate with a semicircular notch 10 mm in diameter enclosing the surface of the sample. The sample was mounted on a shaft driven by an electric motor. The counter body was mounted on a platform sliding along cylindrical guides. The platform was moved using a pneumatic cylinder. The cylinder, guides and the platform were able to rotate with the pendulum. The pendulum shaft was located coaxially with the sample. Such a scheme makes it possible to preserve the common rotation axis for the sample and the counter body as they exhaust and to avoid the influence of misalignment on the results of measurements of the frictional moment. Friction tests were carried out in dry friction mode under a load of 10 N. The sliding speed of the sample along the counter body was 1.555 m/s. The friction path was 1000 m. The parameters of the microgeometry of the friction tracks' surface were measured using the TR200 profilometer (Beijing TIME High

 doi:10.20944/preprints202306.1529.v1

Technology Ltd., Beijing, China). The temperature of the friction contact was measured on the friction track directly at the exit from the contact area using the MLX90614 digital infrared thermometer (Melexis Electronic Technology, Shanghai, China). Friction parameters of the worn surface after PENC and PEP were calculated using a model previously adapted for similar coatings [34].

3. Results

3.1. Morphology, Structure and Tribological Properties of the Surface after PENC

Morphological analysis of the titanium alloy surface after PENC demonstrated the effect the treatment temperature has on the condition of the surface (Figure 4). At a low temperature of PENC, the formation of thin oxide films is observed, the overlap area of which on the surface increases with an increase in temperature from 750 to 800 °C. After treatment at a temperature of 850 °C, the formation of a porous structure of the oxide layer is observed with a tendency for pore growth as the temperature increases to 900 °C.

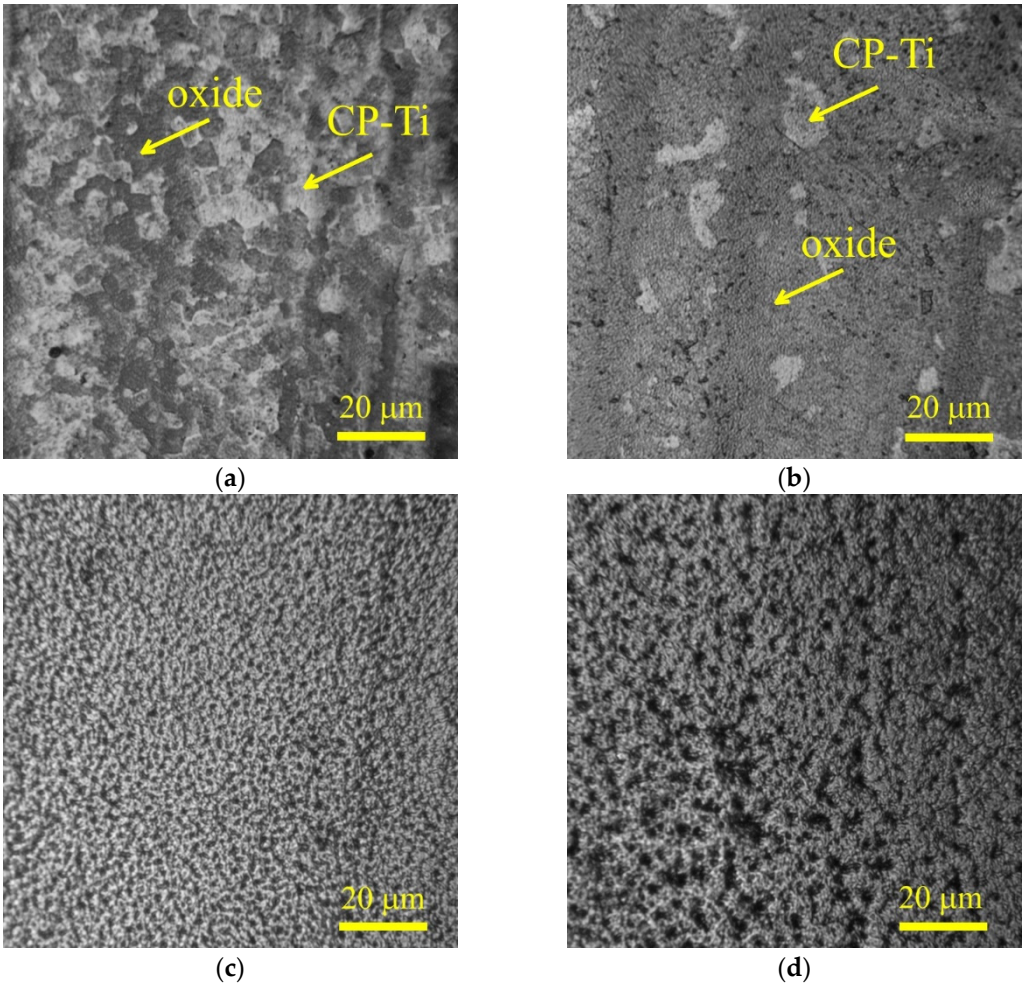

Figure 4. Morphology of the CP-Ti surface after PENC at different treatment temperature: (**a**) 750 °C; (**b**) 800 °C; (**c**) 850 °C; (**d**) 900 °C.

The change in the surface morphology affected its roughness (Table 1). Follwoing PENC, a decrease in surface roughness *Ra* is observed due to the electrochemical dissolution of irregularities, which is characteristic of anodic processes [13,15,28,31,33]. The formation of a porous structure of the oxide layer at a treatment temperature of 900 °C is reflected in an increase in roughness, which does not exceed the initial value.

Preprints (www.preprints.org) | NOT PEER-REVIEWED | Posted: 21 June 2023 doi:10.20944/preprints202306.1529.v1

Table 1. Values of surface roughness *Ra*; average friction coefficient over the last 100 m of the path with friction μ per 1 km; friction track temperature over the last 100 m of the path at friction T_{fr} per 1 km; weight loss during friction at 1 km of the path Δm_{fr}; magnitude of the absolute penetration in the tribocontact *h*; relative penetration of the deformed surfaces of the tribocontact *h*/*r*; Kragelsky–Kombalov criterion Δ of CP-Ti samples after PENC at different temperatures *T*.

T (°C)	*Ra* (μm)	μ	T_{fr} (°C)	Δm_{fr} (mg)	*h* (μm)	*h*/*r*	Δ
Untreated	1.00 ± 0.10	0.465±0.005	56.0	3.70±0.04	0.150	0.062	0.58
750	0,61±0,15	0.318±0.003	53.3	0.85±0.01	0.131	0.052	0.51
800	0,57±0,14	0.428±0.004	65.0	1.45±0.02	0.134	0.058	0.52
850	0,55±0,14	0.421±0.004	87.0	3.75±0.04	0.130	0.051	0.52
900	0,80±0,12	0.417±0.004	90.9	6.50±0.08	0.136	0.050	0.54

Metallographic analysis of the cross-section of the samples showed the formation of a diffusion layer under the oxide layer (Figure 5).

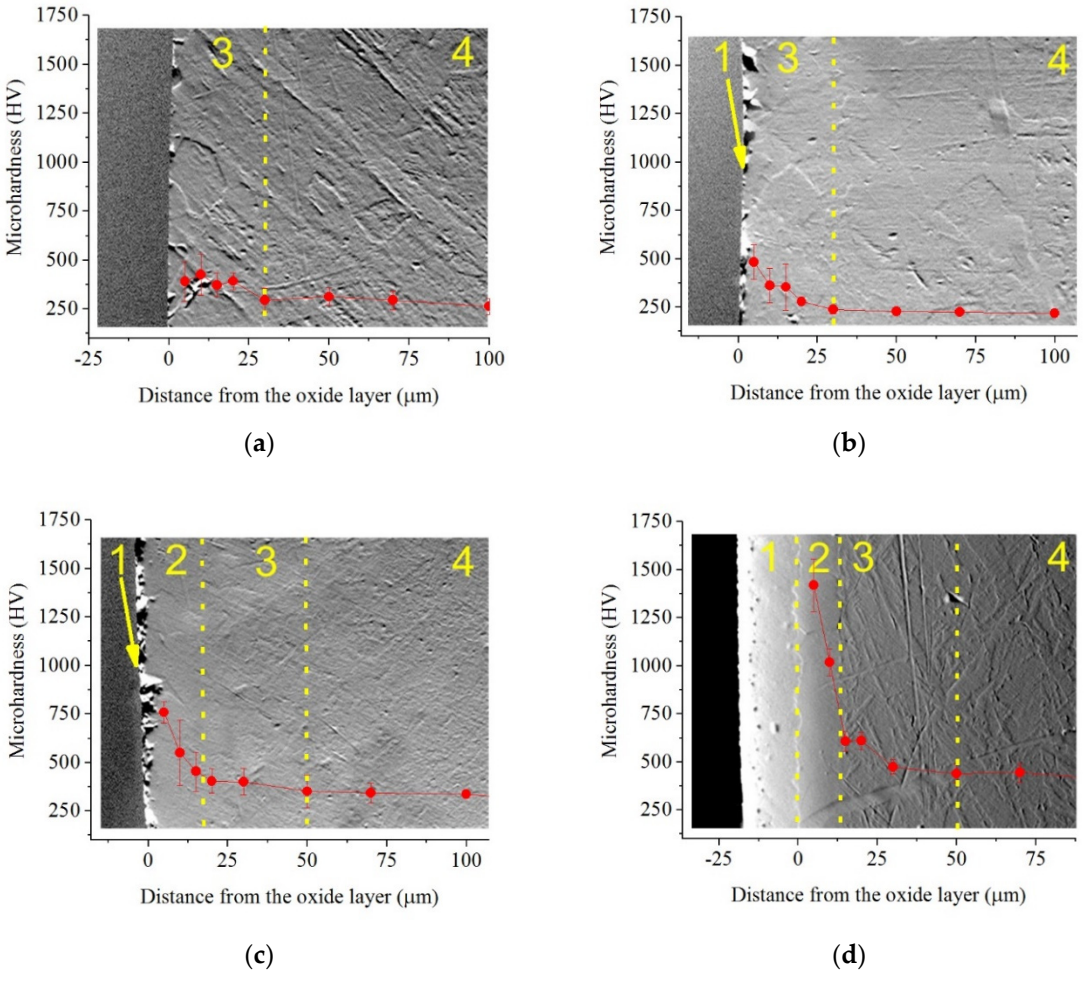

Figure 5. SEM image of cross-section of the CP-Ti surface after PENC and microhardness distribution at different treatment temperature: (**a**) 750 °C; (**b**) 800 °C; (**c**) 850 °C; (**d**) 900 °C. 1—oxide layer; 2—outer hardened layer; 3—diffusion layer; 3—initial structure.

The above described surface morphology correlates with the thickness of the oxide layer, which is visually determined at temperatures of 800, 850, and 900 °C and tends to increase as temperature rises. The diffusion layer, which is a solid solution of nitrogen and carbon, is determined by an increase in microhardness by 200–250 HV. At temperatures of 850 and 900°C, a hardened layer is

Preprints (www.preprints.org) | NOT PEER-REVIEWED | Posted: 21 June 2023 doi:10.20944/preprints202306.1529.v1

detected metallographically with a significant increase in microhardness (outer hardened layer), achieved after 900 °C to 1280 HV, and 5 times higher than the microhardness of the initial structure.

Tribological tests have shown the possibility of reducing the friction coefficient of the surface of the titanium alloy CP-Ti after PENC, which is minimal after treatment at 750 °C (Table 1, Figure 6). Weight wear decreases after PENC at 750 and 800 °C. At the same time, a linear increase in weight wear has been observed when increasing the treatment temperature. A similar trend is observed for the temperature in the friction contact zone, which decreases only after PENC at 750 °C and rises as the treatment temperature rises.

To determine the stress-strain state of the contact, as well as the wear mechanism, the relative convergence of the rubbing surfaces was found, based on the profilograms of the friction tracks. According to the calculation of the relative penetration of the asperities of the compressed surfaces h/r (the ratio of the depth of the penetration of the asperity into the surface of the counterbody to the radius of the asperity), in the untreated and nitrocarburized samples, the friction bonds during friction are destroyed due to the plastic displacement of the material ($0.01 < h/r < 0.1$). The roughness on the friction tracks, evaluated after the complex criterion of Kragelsky-Kombalov, decreased for nitrocarburized samples. In this case, the correlation of the complex criterion with the surface roughness before tribological tests can be observed.

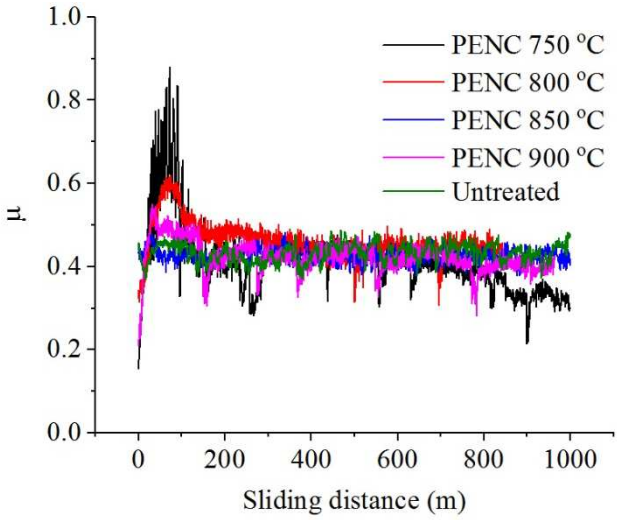

Figure 6. Dependence of friction coefficient on sliding distance of the untreated and PENC samples.

3.2. Morphology and Tribological Properties of the Surface after PEP

Following PENC at 900 °C, the samples were subjected to subsequent PEP, which demonstrated high hardness levels, and the removal of fragile parts of the oxide layer, which are destroyed during friction, will allow to improve the tribological properties, as was demonstrated in the duplex treatment of steels [35,36].

The results of profilometric studies showed that after PEP in a sulfate electrolyte, a slight increase in roughness occurs within the measurement error without revealing dependences on the PEP voltage and time (Table 2). In this case, the minimum material removal rate is observed, caused by additional passivation of the surface by oxygen-containing sulfate ions.

Preprints (www.preprints.org) | NOT PEER-REVIEWED | Posted: 21 June 2023 doi:10.20944/preprints202306.1529.v1

Table 2. Values of weight loss Δm; surface roughness Ra; average friction coefficient over the last 100 m of the path with friction μ per 1 km; friction track temperature over the last 100 m of the path at friction T_{fr} per 1 km; weight loss during friction at 1 km of the path Δm_{fr}; volume loss during friction at 1 km of the path ΔV_{fr}; magnitude of the absolute penetration in the tribocontact h; relative penetration of the deformed surfaces of the tribocontact h/r; Kragelsky–Kombalov criterion Δ of CP-Ti samples after PENC at 900 °C and subsequent PEP in a solution of ammonium sulfate (3%) at different voltage U and time t.

U (V)	t (min)	Δm (mg)	Ra (μm)	μ	T_{fr} (°C)	Δm_{fr} (mg)	ΔV_{fr} (mm³)	h (μm)	h/r	Δ
Untreated			1.00 ± 0.10	0.465	56	3.70	5.62	0.150	0.062	0.58
PENC at 900 °C			0.80 ± 0.12	0.417	91	6.50	7.94	0.136	0.050	0.54
275	1	1.4	0.86 ± 0.10	0.467	130	2.83	3.02	0.158	0.069	0.56
	3	4.0	0.89 ± 0.07	0.413	116	2.65	2.99	0.155	0.067	0.53
	5	4.7	0.89 ± 0.08	0.257	114	1.14	1.08	0.123	0.048	0.44
	10	6.4	1.09 ± 0.12	0.249	102	0.82	1.02	0.121	0.044	0.40
300	1	2.8	0.87 ± 0.07	0.292	110	0.93	1.12	0.131	0.053	0.48
	3	4.7	0.90 ± 0.08	0.304	113	0.90	1.14	0.135	0.057	0.49
	5	6.5	0.89 ± 0.13	0.299	111	0.90	1.04	0.132	0.055	0.48
	10	9.6	0.85 ± 0.06	0.262	108	0.90	0.98	0.131	0.054	0.45
325	1	3.9	0.94 ± 0.04	0.362	107	1.11	1.28	0.134	0.058	0.50
	3	4.3	0.92 ± 0.10	0.374	106	1.21	1.24	0.135	0.060	0.51
	5	7.1	0.87 ± 0.09	0.372	108	1.10	1.26	0.136	0.060	0.51
	10	9.9	0.85 ± 0.06	0.360	106	1.17	1.30	0.135	0.058	0.50

Morphological analysis showed that the surface becomes more uniform due to the removal of the bulges with PEP (Figure 7b).

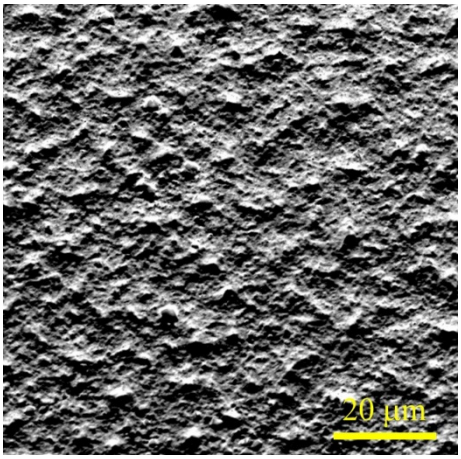

(**a**)

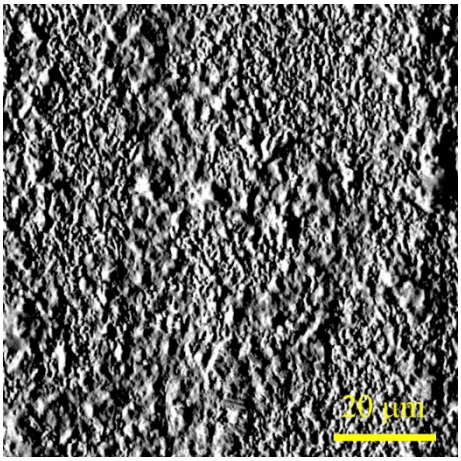

(**b**)

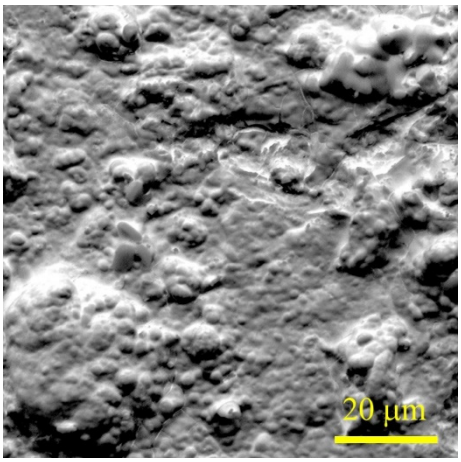

(**c**)

(**d**)

Preprints (www.preprints.org) | NOT PEER-REVIEWED | Posted: 21 June 2023 doi:10.20944/preprints202306.1529.v1

Figure 7. Morphology of the CP-Ti surface after: (**a**) PENC at 900 °C; (**b**) PEP in a solution of ammonium sulfate (3%) at 300 V for 3 min; (**c**) PEP in a solution of ammonium chloride (1%) at 300 V for 3 min; (**d**) PEP in a solution of ammonium fluoride (4%) at 300 V for 3 min.

PEP in an ammonium sulfate solution, despite a slight increase in roughness, showed the possibility of reducing the friction coefficient, weight and volume wear, possibly caused by the removal of an unstable outer oxide layer during PEP and the formation of oxides in its place under the passivating action of sulfate ions (Table 2, Figure 8). The best results were obtained after PEP at 300 V regardless of the treatment time and at 275 V for at least 5 min. Thus, the value of weight wear can be reduced by 7.9 times compared to nitrocarburized and by 4.5 times compared to the untreated surface, volume wear by 7.8 and 5.5, and the friction coefficient by 1.7 and 1.9 times respectively after PEP at 275 V for 10 min. The temperature in the friction contact zone in all cases exceeds 100 °C. The relative penetration after PEP in any mode for dry friction conditions lies within $0.01 < h/r < 0.1$, which means that plastic deformations were realized in the tribocontact, providing a rather mild friction mode without microcutting. It is demonstrated that the minimum values of the Kragelsky-Kombalov criterion correlate with the minimum values of the friction coefficient.

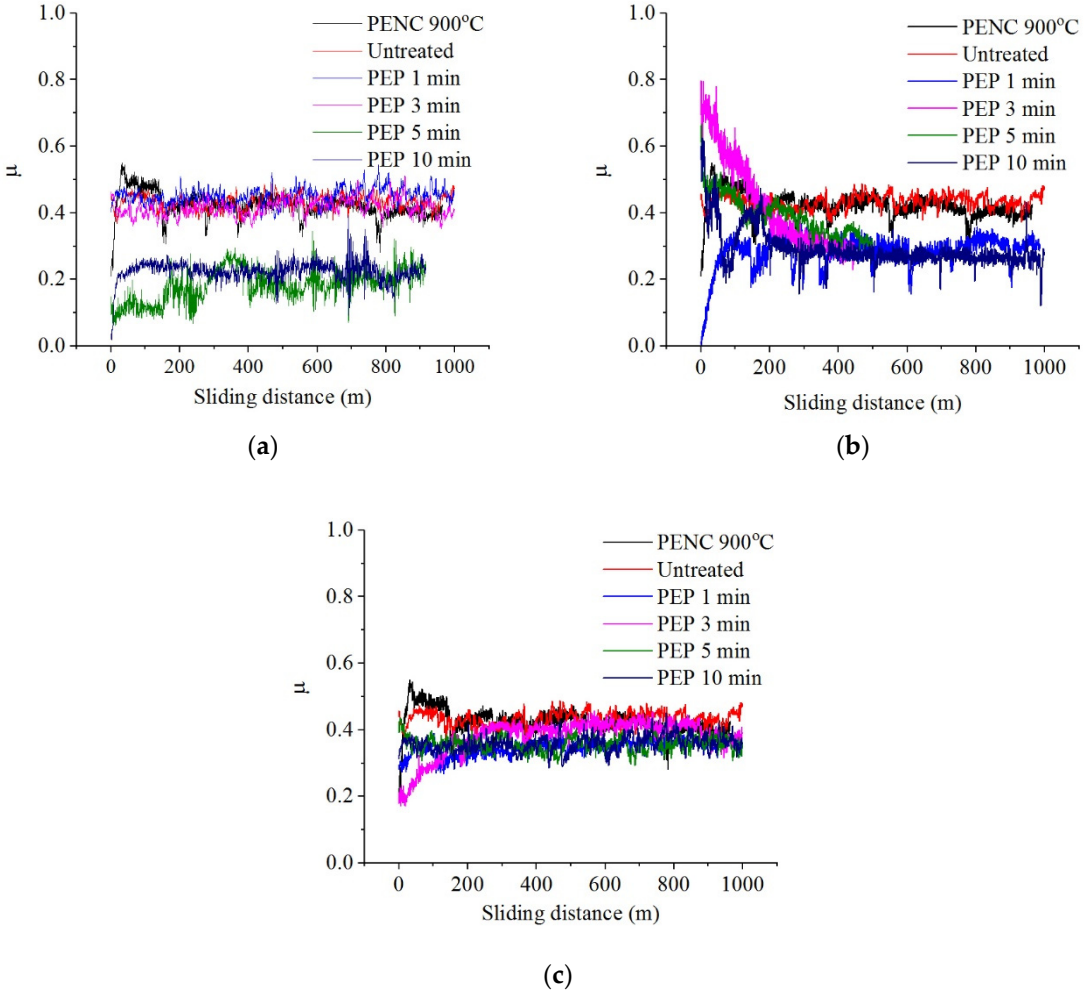

Figure 8. Dependence of friction coefficient on sliding distance of the untreated and treated samples after PENC at 900 °C and subsequent PEP in a solution of ammonium sulfate (3%) at different time and voltage: (**a**) 275 V; (**b**) 300 V; (**c**) 325 V.

When using a chloride electrolyte, a significant increase in roughness is observed in proportion to the PEP duration, regardless of the magnitude of the applied voltage (Table 3). The removal of the

Preprints (www.preprints.org) | NOT PEER-REVIEWED | Posted: 21 June 2023 doi:10.20944/preprints202306.1529.v1

outer oxide layer occurs at a higher rate than during PEP in a sulfate electrolyte, which leads to the development of surface profile irregularities (Figure 7c) and an increase in roughness.

Table 3. Values of weight loss Δm; surface roughness Ra; average friction coefficient over the last 100 m of the path with friction μ per 1 km; friction track temperature over the last 100 m of the path at friction T_{fr} per 1 km; weight loss during friction at 1 km of the path Δm_{fr}; volume loss during friction at 1 km of the path ΔV_{fr}; magnitude of the absolute penetration in the tribocontact h; relative penetration of the deformed surfaces of the tribocontact h/r; Kragelsky–Kombalov criterion Δ of CP-Ti samples after PENC at 900 °C and subsequent PEP in a solution of ammonium chloride (1%) at different voltage U and time t.

U (V)	t (min)	Δm (mg)	Ra (μm)	μ	T_{fr} (°C)	Δm_{fr} (mg)	ΔV_{fr} (mm³)	h (μm)	h/r	Δ
Untreated			1.00 ± 0.10	0.465	56	3.70	5.62	0.150	0.062	0.58
PENC at 900 °C			0.80 ± 0.12	0.417	91	6.50	7.94	0.136	0.050	0.54
275	1	12.7	1.69 ± 0.50	0.798	261	8.21	12.32	0.228	0.099	3.05
	3	25.2	3.02 ± 0.56	0.338	100	2.63	4.82	0.131	0.052	0.51
	5	35.2	5.52 ± 1.08	0.376	120	2.86	4.98	0.138	0.064	0.55
	10	64.9	7.22 ± 1.05	0.382	141	3.08	5.98	0.142	0.066	0.58
300	1	13.0	1.51 ± 0.18	0.773	270	8.05	12.02	0.222	0.080	3.02
	3	20.9	3.11 ± 0.47	0.372	120	2.63	4.51	0.129	0.061	0.50
	5	28.3	4.21 ± 0.34	0.393	133	3.01	5.62	0.129	0.056	0.49
	10	68.1	6.39 ± 0.68	0.435	144	4.08	6.78	0.144	0.068	0.57
325	1	12.0	1.50 ± 0.14	0.811	310	8.40	12.48	0.236	0.096	3.22
	3	26.7	3.20 ± 0.41	0.751	281	7.62	8.92	0.217	0.093	2.97
	5	34.0	4.25 ± 0.47	0.523	150	5.99	7.13	0.148	0.072	0.62
	10	70.8	5.20 ± 0.76	0.622	170	6.12	10.54	0.201	0.092	2.85

PEP in an ammonium chloride solution makes it possible to improve the tribological parameters only after treatment at 275 and 300 V for 3–5 min (Table 3, Figure 9): the friction coefficient, weight and volume wear can be reduced, respectively, by 1.2, 2.5 and 1.8 times compared with nitrocarburized and 1.4, 1.4 and 1.2 times compared to untreated samples. PEP for 1 min at 275 and 300 V, as well as 1, 3 and 10 min at 325 V, showed high temperature readings in the friction contact zone and friction coefficient with relatively high microtopology indicators. Under these conditions, there is a transition in the destruction of friction bonds from soft plastic displacement of the material to microcutting ($h/r \approx 0.1$).

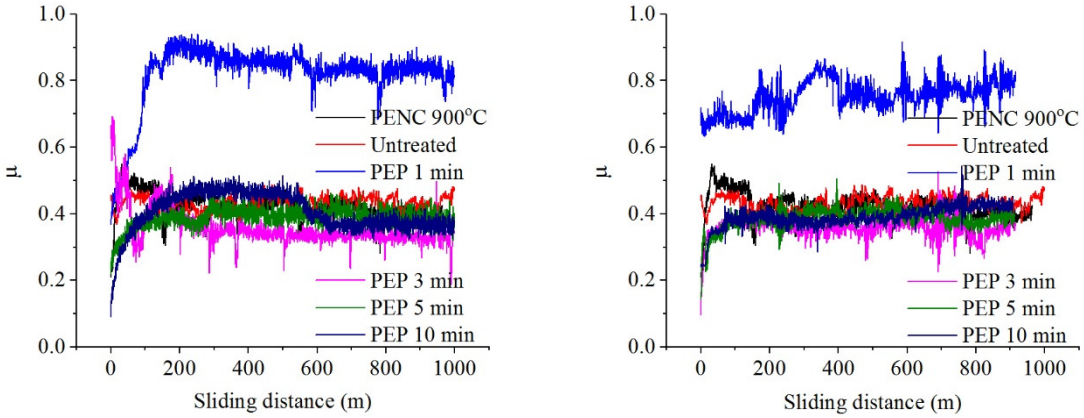

(**a**) (**b**)

Preprints (www.preprints.org) | NOT PEER-REVIEWED | Posted: 21 June 2023 doi:10.20944/preprints202306.1529.v1

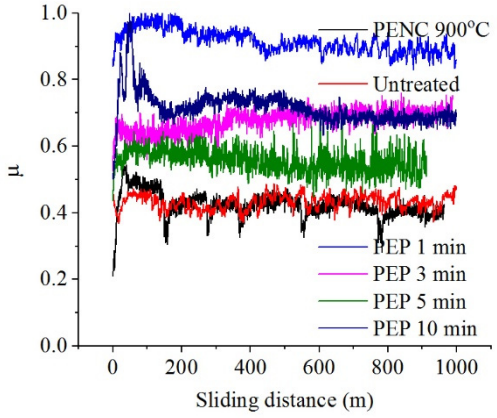

(**c**)

Figure 9. Dependence of friction coefficient on sliding distance of the untreated and treated samples after PENC at 900 °C and subsequent PEP in a solution of ammonium chloride (1%) at different time and voltage: (**a**) 275 V; (**b**) 300 V; (**c**) 325 V.

When using a fluoride electrolyte, the roughness decreases with an increase in PEP duration, and in the case of PEP at 275 and 300 V for more than 3 min, its value drops below the initial value for the PENC surface (Table 4). During PEP in this electrolyte, the greatest loss of material occurs, leading to a uniform removal of the oxide layer according to the morphological analysis data (Figure 7d).

Table 4. Values of weight loss Δm; surface roughness *Ra*; average friction coefficient over the last 100 m of the path with friction μ per 1 km; friction track temperature over the last 100 m of the path at friction T_{fr} per 1 km; weight loss during friction at 1 km of the path Δm_{fr}; volume loss during friction at 1 km of the path ΔV_{fr}; magnitude of the absolute penetration in the tribocontact *h*; relative penetration of the deformed surfaces of the tribocontact *h*/*r*; Kragelsky–Kombalov criterion Δ of CP-Ti samples after PENC at 900 °C and subsequent PEP in a solution of ammonium fluoride (4%) at different voltage *U* and time *t*.

U (V)	*t* (min)	Δ*m* (mg)	*Ra* (μm)	μ	T_{fr} (°C)	Δm_{fr} (mg)	ΔV_{fr} (mm³)	*h* (μm)	*h*/*r*	Δ
Untreated			1.00 ± 0.10	0.465	56	3.70	5.62	0.150	0.062	0.58
PENC at 900 °C			0.80 ± 0.12	0.417	91	6.50	7.94	0.136	0.050	0.54
275	1	17.4	0.95 ± 0.07	0,251	72	0.91	1.03	0.123	0.048	0.44
	3	42.9	0.61 ± 0.05	0,248	76	0.89	0.98	0.121	0.044	0.40
	5	67.1	0.52 ± 0.08	0,225	76	0.80	0.88	0.108	0.043	0.38
300	1	27.4	1.01 ± 0.05	0,355	85	2.33	4.02	0.134	0.054	0.56
	3	52.5	0.75 ± 0.02	0,211	75	0.78	0.74	0.101	0.042	0.32
	5	88.2	0.76 ± 0.02	0,239	74	0.91	1.03	0.122	0.043	0.37
325	1	20.3	1.02 ± 0.02	0,360	80	2.55	4.67	0.135	0.057	0.50
	3	29.6	0.99 ±0.04	0,384	84	2.90	5.44	0.137	0.061	0.53
	5	37.1	0.81 ± 0.01	0.349	82	2.70	5.01	0.133	0.054	0.49

PEP in an ammonium fluoride solution under all varied modes makes it possible to improve the friction and wear characteristics (Table 4, Figure 10). The best results were obtained after PEP at 275 V, regardless of the duration of treatment and at 300 V for 3–5 min: the coefficient of friction, weight and volume wear can be reduced, by 2, 8.3 and 10.7 times respectively compared with nitrocarburized and 2.2, 4.7 and 7.6 times compared to untreated samples after PEP at 300 V for 3 min. The temperatures in the tribological contact after PEP in a fluoride electrolyte are lower than in chloride and sulfate ones. The low values of the Kragelsky-Kombalov criterion indicate an increased bearing capacity of the rough profile following this treatment, which is also evident from the low values of the friction coefficient. A small difference between the Δ criterion and the roughness after PEP provides running in with the lowest possible mass wear losses.

Preprints (www.preprints.org) | NOT PEER-REVIEWED | Posted: 21 June 2023 doi:10.20944/preprints202306.1529.v1

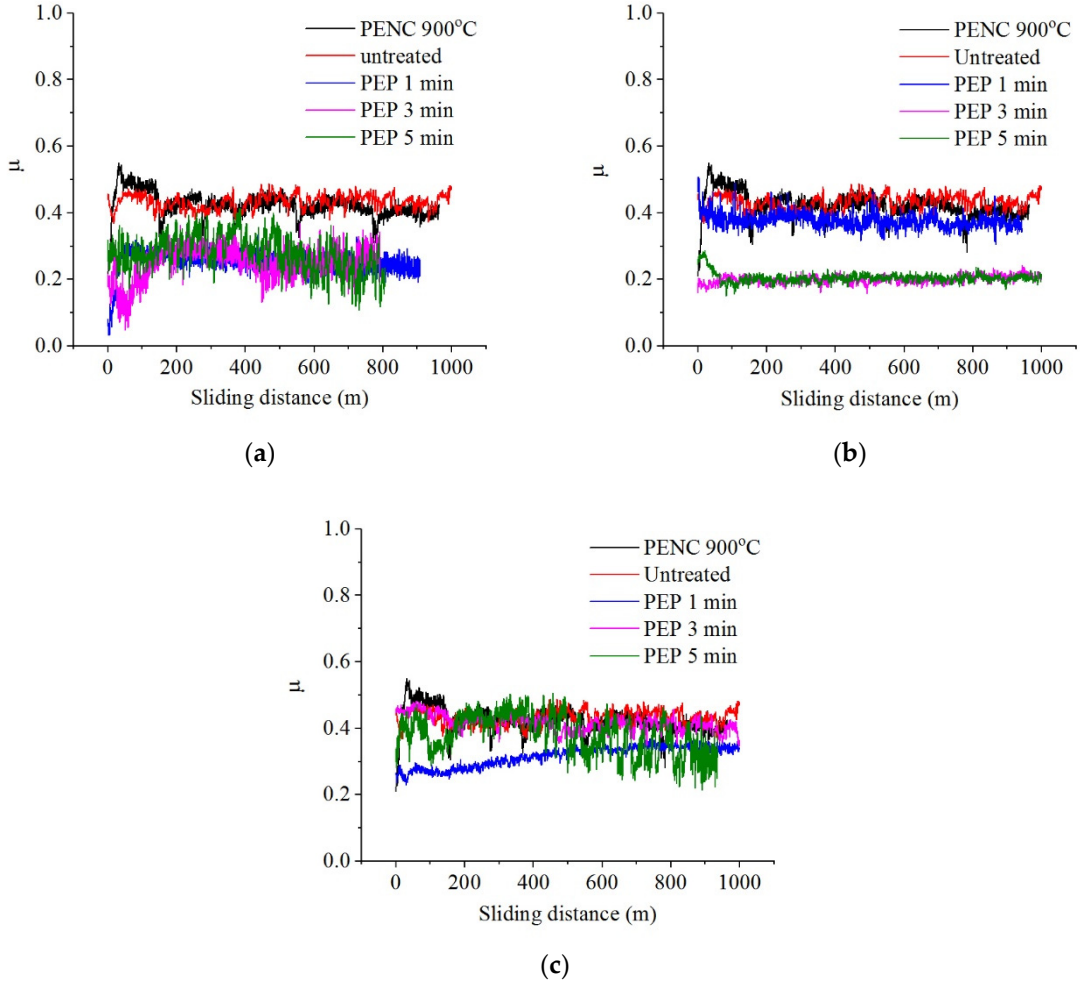

Figure 10. Dependence of friction coefficient on sliding distance of the untreated and treated samples after PENC at 900 °C and subsequent PEP in a solution of ammonium fluoride (4%) at different time and voltage: (**a**) 275 V; (**b**) 300 V; (**c**) 325 V.

The mechanism of sample wear following PEP in a fluoride electrolyte can be described as fatigue in dry friction and plastic contact ($0.01 < h/r < 0.1$).

4. Discussion

The results of the morphological analysis of the surface showed a competing effect of high-temperature oxidation of the surface and its anodic dissolution, which proves the general similarity of the anodic diffusion saturation of steels [13,19,28,31,33] and titanium alloys [15,29]. When treated at up to 900 °C, anodic dissolution prevails over oxidation and the roughness decreases by almost two-fold. With an increase in temperature to 900 °C, evenly formed irregularities of the oxide coating are revealed on the surface, leading to an increase in roughness. In this case, oxidation prevails over anodic dissolution. Similar to the diffusion saturation of steels [28,31,33], nitrocarburizing of CP-Ti results in the formation of diffusion layers with increased hardness, which increases with rising treatment temperature.

Tribological testing of nitrocarburized surfaces revealed a negative effect of the outer oxide layer on wear characteristics. The observed increase in weight wear with an increase in the PENC temperature is caused by the destruction of the outer oxide layer during triboconjugation, the thickness and uneven development of which increase with the prevalence of high-temperature oxidation. With an increase in the treatment temperature, the bond between the oxides and the base metal is weakened due to different coefficients of thermal expansion, and the oxides easily peel off

 doi:10.20944/preprints202306.1529.v1

during friction. The oxide flaking zone can extend beyond the friction track, thereby increasing the mass loss during tribological tests. An increase in temperature in the zone of frictional contact with a similar dependence can be attributed to the increase in the hardness of the diffusion layers and the strength of the adhesive bonds of the sample material on the cut.

The use of the methodology [34] for describing the stress-strain state of the contact of rubbing surfaces and establishing the wear mechanism can be substantiated as follows. Each passing of the surface roughness of the PENC sample over the surface of the counterbody is characterized by residual deformation. The accumulation of residual strains in the near-surface layers of both the sample and the counterbody leads to the emergence of a stress state characterized by low-cycle frictional fatigue of the material. Microscopic sections of the material begin to break off, forming wear particles. The intensity of formation of wear particles is determined by the stage of the wear process, which can be determined by the transition of the initial roughness to the operational one. After the running-in process is complete, a roughness is formed on the friction surfaces of the PENC sample and the counterbody, which is determined only by the conditions of friction and wear. The resulting roughness is optimal for a given tribological assembly and friction conditions and results in minimal wear. It may be greater or less than the roughness value prior to friction testing. This roughness is called equilibrium and is measured by a dimensionless complex parameter using the Kragelsky-Kombalov criterion Δ. This is what will be reproduced during the period of stationary wear during the subsequent interaction of the friction pair and characterize the bearing capacity of the surface. The more the initial roughness of the friction surface determined by *Ra* differs from the optimal one, estimated using the Kragelsky-Kombalov criterion Δ, the greater the wear during the running-in period will be, which is one of the components of the total wear for the entirety of the friction test.

Based on the revealed positive complex effect of high hardness of the surface layer and low surface roughness [24], it was proposed to carry out PEP of samples with the highest surface layer hardness, along with the poor performance in terms of roughness and surface morphology.

The use of electrolytes for PEP with various anions demonstrated a similar trend with the polishing of diffusion-saturated steels using sulfate and ammonium chloride [35,36]. PEP in a sulfate electrolyte leads to the formation of a more uniform surface due to the removal of the loose oxide layer and the formation of denser oxide structures in its place under the passivating action of sulfate ions. This leads to the increase in temperature in the zone of frictional contact. The formation of a morphologically homogeneous dense structure of the oxide layer results in an increase in wear resistance. It was found that after PEP in a sulfate electrolyte, the bearing capacity of the friction track profile in tribological contact, which is estimated by the Kragelsky-Kombalov criterion (the lower its value, the higher the bearing capacity), increases. As can be seen from Table 2, PEP at a voltage of 300 V and 275 V (5 and 10 min) provide the maximum bearing capacity of the profile in friction tests, which is confirmed by the minimum values of the friction coefficients for these conditions. PEP in a chloride electrolyte, as in the case of complex processing of steels, leads to an increase in surface inhomogeneity and its roughness. This is also reflected in the decrease in tribological properties. The bearing capacity of such a surface decreases, and under certain processing conditions, the destruction of friction bonds changes from soft plastic displacement to microcutting.

In contrast to the duplex treatment of steel surfaces, it was proposed to carry out PEP of CP-Ti after PENC in a fluoride electrolyte. A more intensive removal of the oxide layer and the formation of a uniform surface with a low roughness value is shown. Such a surface with a retained diffusion layer with high hardness leads to the formation of a friction surface profile with a high bearing capacity. This is reflected in the lower values of the coefficient of friction, mass and volume wear compared to the use of sulfate and ammonium chloride-based.

5. Conclusions

The structure, morphology, roughness, and tribological characteristics of the surface of CP-Ti after PENC and subsequent PEP in various electrolytes and conditions have been studied:

(a) The morphologically uniform surface typical of anodic processes and the dependence of surface roughness on PENC temperature is demonstrated, determined by the competition between

high-temperature oxidation and anodic dissolution, which smoothes surface irregularities and reduces roughness.

(b) It is demonstrated that PEP in a chloride electrolyte leads to an uneven surface etching and an increase in its roughness, as was observed for steel samples, and so its use to reduce roughness is not practical. When plasma electrolytic polishing a nitrocarburized CP-Ti in a sulfate electrolyte, there is no decrease in roughness, neither a significant increase: there is additional oxidation of the surface and minimal material removal at a rate of (1.3 ± 0.2) mg/min. Positive results in reducing roughness are shown with PEP in a fluoride electrolyte (4%) at a temperature of 90 °C at 250 and 300 V for 3–5 min, reflected in the uniform removal of oxide layer irregularities with a high material removal rate equal to (16.8 ± 2.5) mg/min.

(c) The results of tribological tests in dry friction of the lateral surface of a cylindrical sample on a disk made of tool steel under a load of 10 N, a linear sliding velocity of the sample of 1.555 m/s on a friction path of 1 km showed the possibility of reducing the friction coefficient and weight wear of the surface of CP-Ti after PENC. The correlation of weight wear with the hardness of the hardened layer at a low treatment temperature and the thickness of the oxide layer was established: the largest decrease in weight wear occurs after PENC at 750 °C for 5 min (by 4.3 times).

(d) The possibility of further increase in wear resistance by subsequent PEP of nitrocarburized CP-Ti at a voltage of 275–300 V for 3–5 min in chloride and fluoride electrolytes and 5–10 min in sulfate electrolyte was revealed. This leads to a decrease in the friction coefficient, weight and volume wear. Under these conditions, the hardened layer is preserved when the porous outer oxide layer is removed.

(e) According to the microtopology of the friction tracks, the wear mechanism under optimal conditions of PENC and PEP is fatigue under plastic contact and dry friction.

Author Contributions: Conceptualization, S.K. and S.G.; methodology, T.M., I.T., I.K. and S.Sh.; validation, S.K., I.S. and M.K.; formal analysis, I.K. and S.Sh.; investigation, T.M., I.T., R.B. and R.N.; resources, S.K., I.S. and S.G.; writing—original draft preparation, S.K., I.K., I.S.; writing—review and editing, S.K., M.K. and S.G.; visualization, T.M., I.T., S.Sh.; supervision, S.K.; project administration, I.S.; funding acquisition, S.G. All authors have read and agreed to the published version of the manuscript.

Funding: This work is funding by the state assignment of the Ministry of Science and Higher Education of the Russian Federation, Project No. FSFS-2021-0006. The study was carried out on the equipment of the Center of collective use of MSUT "STANKIN" supported by the Ministry of Higher Education of Russian Federation.

Institutional Review Board Statement: Not applicable.

Informed Consent Statement: Not applicable.

Data Availability Statement: Not applicable.

Conflicts of Interest: The authors declare no conflict of interest.

References

1. Yin, F.; Hu, S.; Xu, R.; Han, X.; Qian, D.; Wei, W.; Hua, L.; Zhao, K. Strain rate sensitivity of the ultrastrong gradient nanocrystalline 316L stainless steel and its rate-dependent modeling at nanoscale. Int. J. Plast. 2020, 129, 102696. https://doi.org/10.1016/j.ijplas.2020.102696.
2. Li, P.; Hu, S.; Liu, Y.; Hua, L.; Yin, F. Surface Nanocrystallization and Numerical Modeling of 316L Stainless Steel during Ultrasonic Shot Peening Process. Metals 2022, 12, 1673. https://doi.org/10.3390/met12101673.
3. Chen, Y.; Deng, S.; Zhu, C.; Hu, K.; Yin, F. The effect of ultrasonic shot peening on the fatigue life of alloy materials: A review. Int. J. Comput. Mater. Sci. Surf. Eng. 2021, 10, 209–234. https://doi.org/10.1504/IJCMSSE.2021.121360.
4. Yerokhin, A.L.; Nie, X.; Leyland, A.; Matthews, A.; Dowey, S. Plasma electrolysis for surface engineering. Surf. Coat. Technol. 1999, 122, 73–93. https://doi.org/10.1016/S0257-8972(99)00441-7
5. Mora-Sanchez, H.; Pixner, F.; Buzolin, R.; Mohedano, M.; Arrabal, R.; Warchomicka, F.; Matykina, E. Combination of Electron Beam Surface Structuring and Plasma Electrolytic Oxidation for Advanced Surface Modification of Ti6Al4V Alloy. Coatings 2022, 12, 1573. https://doi.org/10.3390/coatings12101573.

6. Perez, H.; Vargas, G.; Magdaleno, C.; Silva, R. Article: Oxy-Nitriding AISI 304 Stainless Steel by Plasma Electrolytic Surface Saturation to Increase Wear Resistance. Metals 2023, 13, 309. https://doi.org/10.3390/met13020309.
7. Marcuz, N.; Ribeiro, R.P.; Rangel, E.C.; Cristino da Cruz, N.; Correa, D.R.N. The Effect of PEO Treatment in a Ta-Rich Electrolyte on the Surface and Corrosion Properties of Low-Carbon Steel for Potential Use as a Biomedical Material. Metals 2023, 13, 520. https://doi.org/10.3390/met13030520.
8. Aliofkhazraei, M.; Macdonald, D.D.; Matykina, E.; Parfenov, E.V.; Egorkin, V.S.; Curran, J.A.; Troughton, S.C.; Sinebryukhov, S.L.; Gnedenkov, S.V.; Lampke, T.; Simchen, F.; Nabavi, H.F. Review of plasma electrolytic oxidation of titanium substrates: Mechanism, properties, applications and limitations. Appl. Surf. Sci. Advances 2021, 5, 100121. https://doi.org/10.1016/j.apsadv.2021.100121.
9. Jin, S.; Ma, X.; Wu, R.; Wang, G.; Zhang, J.; Krit, B.; Betsofen, S.; Liu, B. Advances in micro-arc oxidation coatings on Mg-Li alloys. Appl. Surf. Sci. Advances 2022, 8, 100219. https://doi.org/10.1016/j.apsadv.2022.100219.
10. Bogdashkina, N.L.; Gerasimov, M.V.; Zalavutdinov, R.K.; Kasatkina, I.V.; Krit, B.L.; Lyudin, V.B.; Fedichkin, I.D.; Shcherbakov, A.I.; Apelfeld, A.V. Influence of Nickel Sulfate Additives to Electrolytes Subjected to Microarc Oxidation on the Structure, Composition, and Properties of Coatings Formed on Titanium. Surf. Eng. Appl. Electrochem. 2018, 54, 331–337. https://doi.org/10.3103/S106837551804004X.
11. Belkin, P.N.; Kusmanov, S.A.; Parfenov, E.V. Mechanism and technological opportunity of plasma electrolytic polishing of metals and alloys. Appl. Surf. Sci. Adv. 2020, 1, 100016. https://doi.org/10.1016/j.apsadv.2020.100016.
12. Belkin, P.N.; Yerokhin, A.L.; Kusmanov, S.A. Plasma Electrolytic Saturation of Steels with Nitrogen and Carbon. Surf. Coat. Technol. 2016, 307, 1194–1218. https://doi.org/10.1016/j.surfcoat.2016.06.027.
13. Belkin, P.N.; Kusmanov, S.A. Plasma electrolytic nitriding of steels. J. Surf. Investig. X-ray Synchrotron Neutron Tech. 2017, 11, 767–789. https://doi.org/10.1134/S1027451017020045.
14. Kusmanov, S.A.; Tambovskiy, I.V.; Kusmanova, I.A.; Belkin, P.N. Some features of anodic plasma electrolytic processes in aqueous solution. J. Phys.: Conf. Ser. 2019, 1396, 012025. https://doi.org/10.1088/1742-6596/1396/1/012025.
15. Belkin, P.N.; Kusmanov, S.A.; Zhirov, A.V.; Belkin, V.S.; Parfenyuk, V.I. Anode Plasma Electrolytic Saturation of Titanium Alloys with Nitrogen and Oxygen. J. Mat. Sci. Tech. 2016, 32, 1027–1032. https://doi.org/10.1016/j.jmst.2016.06.005.
16. Nie, X.; Wang, L.; Yao, Z.C.; Zhang, L.; Cheng, F. Sliding wear behaviour of electrolytic plasma nitrided cast iron and steel. Surf. Coat. Technol. 2005, 200, 1745–1750. https://doi.org/10.1016/j.surfcoat.2005.08.046.
17. Taheri, P.; Dehghanian, Ch.; Aliofkhazraei, M.; Rouhaghdam, A.S. Evaluation of Nanocrystalline Microstructure, Abrasion, and Corrosion Properties of Carbon Steel Treated by Plasma Electrolytic Boriding. Plasma Process. Polym. 2007, 4, S711–S716. https://doi.org/10.1002/ppap.200731803.
18. Kuzenkov, S.E.; Saushkin, B.P. Borating of steel 45 in electrolytic plasma. Surf. Eng. Appl. Electrochem. 1996, 6, 10–15.
19. Kusmanov, S.A.; Tambovskiy, I.V.; Sevostyanova, V.S.; Savushkina, S.V.; Belkin, P.N. Anode plasma electrolytic boriding of medium carbon steel. Surf. Coat. Technol. 2016, 291, 334–341. https://doi.org/10.1016/j.surfcoat.2016.02.062.
20. Aliofkhazraei, M.; Taheri, P.; Sabour Rouhaghdam, A.; Dehghanian, C. Study of nanocrystalline plasma electrolytic carbonitriding for CP-Ti. Mater. Sci. 2007, 43, 791–799. https://doi.org/10.1007/s11003-008-9055-5.
21. Dong, Y.-X.; Chen, Y.-S.; Chen, Q.; Liu, B.; Song, Z.-X. Characterization and blood compatibility of TiCxN1−x hard coating prepared by plasma electrolytic carbonitriding. Surf. Coat. Technol. 2007, 201, 8789–8795. https://doi.org/10.1016/j.surfcoat.2007.05.097.
22. Hu, Z.; Xie, F.; Liu, Y.; Wu, X. Study of plasma electrolytic nitrocarburizing on surface of titanium alloy. Materials review 2008, 04. http://en.cnki.com.cn/Article_en/CJFDTOTAL-CLDB200804037.htm.
23. Li, X.-M.; Han, Y. Mechanical properties of Ti(C0.7N0.3) film produced by plasma electrolytic carbonitriding of Ti6Al4V alloy. Appl. Surf. Sci. 2008, 254, 6350–6357. https://doi.org/10.1016/j.apsusc.2008.03.172.
24. Kusmanov, S.A.; Tambovskii, I.V.; Korableva, S.S.; Mukhacheva, T.L.; D'yakonova, A.D.; Nikiforov, R.V.; Naumov, A.R. Wear resistance increase in Ti6Al4V titanium alloy using a cathodic plasma electrolytic nitriding. Surf. Eng. Appl. Electrochem. 2022, 58, 451–455. https://doi.org/10.3103/S1068375522050088.

25. Aliofkhazraei, M.; Rouhaghdam, A. S.; Denshmaslak, A.; Jafarian, H. R.; Sabouri, M. Study of bipolar pulsed nanocrystalline plasma electrolytic carbonitriding on nanostructure of compound layer for CP-Ti. J. Coat. Technol. Res. 2008, 5, 497–503. https://doi.org/10.1007/s11998-008-9086-8.
26. Aliev, M.Kh.; Sabour, A.; Taheri, P. Corrosion Protection Study of Nanocrystalline Plasma-Electrolytic Carbonitriding Process for CP-Ti. Prot. Met. Phys. Chem. Surf. 2008, 44, 618–623. https://doi.org/10.1134/S0033173208060155.
27. Kong, J.H.; Okumiya, M.; Tsunekavwa, Y.; Takeda, T.; Yun, K.Y.; Yoshida, M.; Kim, S.G. Surface Modification of SCM420 Steel by Plasma Electrolytic Treatment. Surf. Coat. Technol. 2013, 232, 275–282. https://doi.org/10.1016/j.surfcoat.2013.05.010.
28. Kusmanov, S.A.; Kusmanova, Y.V.; Smirnov, A.A.; Belkin, P.N. Modification of steel surface by plasma electrolytic saturation with nitrogen and carbon. Mater. Chem. Phys. 2016, 175, 164–171. https://doi.org/10.1016/j.matchemphys.2016.03.011.
29. Belkin, P.N.; Borisov, A.M.; Kusmanov, S.A. Plasma Electrolytic Saturation of Titanium and Its Alloys with Light Elements. J. Surf. Investig. X-ray Synchrotron Neutron Tech. 2016, 10, 516–535. https://doi.org/10.1134/S1027451016030058.
30. Kusmanov, S.; Tambovskiy, I.; Silkin, S.; Nikiforov, R.; Belov, R. Increasing the Hardness and Corrosion Resistance of the Surface of CP-Ti by Plasma Electrolytic Nitrocarburising and Polishing. Materials 2023, 16, 1102. https://doi.org/10.3390/ma16031102.
31. Tambovskiy, I.; Mukhacheva, T.; Gorokhov, I.; Suminov, I.; Silkin, S.; Dyakov, I.; Kusmanov, S.; Grigoriev, S. Features of Cathodic Plasma Electrolytic Nitrocarburizing of Low-Carbon Steel in an Aqueous Electrolyte of Ammonium Nitrate and Glycerin. Metals 2022, 12, 1773. https://doi.org/10.3390/met12101773.
32. Kusmanov, S.A.; Dyakov, I.G.; Belkin, P.N.; Gracheva, I.A.; Belkin, V.S. Plasma electrolytic modification of the VT1-0 titanium alloy surface. J. Surf. Investig. X-ray Synchrotron Neutron Tech. 2015, 9, 98–104. https://doi.org/10.1134/S1027451015010139.
33. Kusmanov, S.A.; Kusmanova, Y.V.; Naumov, A.R.; Belkin, P.N. Formation of diffusion layers by anode plasma electrolytic nitrocarburising of low carbon steel. J. Mater. Eng. Perform. 2015, 24, 3187–3193. https://doi.org/10.1007/s11665-015-1578-y.
34. Mukhacheva, T.; Kusmanov, S.; Suminov, I.; Podrabinnik, P.; Khmyrov, R.; Grigoriev, S. Increasing Wear Resistance of Low-Carbon Steel by Anodic Plasma Electrolytic Sulfiding. Metals 2022, 12, 1641. https://doi.org/10.3390/met12101641.
35. Kusmanov, S.; Tambovskiy, I.; Korableva, S.; Silkin, S.; Naumov, A. Modification of Steel Surface by Anodic Plasma Electrolytic Boriding and Polishing. Trans. Indian Inst. Met. 2022, 75, 3185–3192. https://doi.org/10.1007/s12666-022-02719-x.
36. Apelfeld, A.; Borisov, A.; Dyakov, I.; Grigoriev, S.; Krit, B.; Kusmanov, S.; Silkin, S.; Suminov, I.; Tambovskiy, I. Enhancement of Medium-Carbon Steel Corrosion and Wear Resistance by Plasma Electrolytic Nitriding and Polishing. Metals 2021, 11, 1599. https://doi.org/10.3390/met11101599.